Dose-Response:
An International Journal
April-June 2020:1-15

DOI: 10.1177/1559325820923859
journals.sagepub.com/home/dos
SAGE

Two-Step Optimization to Develop a Transdermal Film Loaded With Dapoxetine Nanoparticles: A Promising Technique to Improve Drug Skin Permeation

Tarek A. Ahmed[1,2], Asmaa M. S. Alay[1], Solomon Z. Okbazghi[3], and Nabil A. Alhakamy[1]

Abstract

Dapoxetine (DPX) is an orally administered drug for the treatment of premature ejaculation (PE). One of the challenges of administering DPX orally as a tablet is its poor bioavailability (ie, 42%) due to extensive first-pass metabolism. Thus, it is vital to develop a new formulation and mode of delivery to achieve the unmet needs of PE treatment. In this study, an optimized DPX polymeric nanoparticle (PNP) was developed and subsequently loaded into a transdermal film. The Box–Behnken design was utilized to optimize 3 formulation factors affecting the particle size and entrapment efficiency (EE) of chitosan (CS)-alginate (ALG) PNPs. A 3-level factorial design was used to study the effect of 2 variables affecting DPX cumulative percent released and percent elongation from transdermal films loaded with DPX-PNPs. Permeation parameters were calculated following ex vivo permeation study through rat skin. Transport of the PNPs across the skin layers was investigated using a fluorescence laser microscope. Results revealed that an optimized PNPs formulation was developed with a particle size 415.94 nm and EE 37.31%. Dapoxetine was successfully entrapped in the polymeric matrix. Chitosan and ALG interacted electrostatically with the studied cross-linking agents to form a polyelectrolyte complex. The ex vivo study illustrated a sustained release profile of DPX with enhanced skin permeation from the film loaded PNPs. Moreover, the PNPs was able to penetrate deeper into skin layers. Therefore, DPX transdermal film developed in this work could be considered as a successful drug delivery with better patient compliance for the treatment of PE.

Keywords

dapoxetine, nanoparticles, optimization, transdermal film, skin permeation

Introduction

Pharmaceutical nanotechnology involves the development of small structures with unique physicochemical properties that are characterized by small size and large surface area. These products improve the effectiveness of conventional dosage forms through formulating active pharmaceutical ingredients (APIs) in specific biodegradable nanocarriers such as nanoparticles (NPs), nanocapsules, micellar systems, and conjugates.[1-4] The developed nanocarriers improves therapeutic quality and overcome the drawbacks of conventional treatment.[5] Nanoparticles are solid colloidal particles that may encapsulate, adsorb, or conjugate the active ingredients within a polymeric matrix.[6]The main objectives of using NPs in drug delivery system are to control the particle size and surface properties as well as to maintain drug release with a high therapeutic

[1] Faculty of Pharmacy, Department of Pharmaceutics, King Abdulaziz University, Jeddah, Kingdom of Saudi Arabia
[2] Faculty of Pharmacy, Department of Pharmaceutics and Industrial Pharmacy, Al-Azhar University, Cairo, Egypt
[3] Global Analytical and Pharmaceutical Development, Alexion Pharmaceuticals, New Haven, Connecticut, USA

Received 25 February 2020; received revised 1 April 2020; accepted 10 April 2020

Corresponding Author:
Tarek A. Ahmed, Department of Pharmaceutics, Faculty of Pharmacy, King Abdulaziz University, Jeddah 21589, Kingdom of Saudi Arabia.
Email: tabdelnapy@kau.edu.sa

effect at an optimal rate and dose regimen.[7] Moreover, NPs improve a variety of drug properties, including drug pharmacokinetics, water solubility, bioavailability, and prolong the drug effect through increasing the drug residence time in the body. Nanoparticles can also be developed to permit targeted drug delivery, which reduces potential side effects and increases therapeutic efficiency.[8] Additionally, NPs improve intracellular penetration and prevent enzymatic degradation, thereby increasing the drug stability and helping to maintain the drug's safety profile through increased therapeutic index as well as reduced risks of toxicity.[9] These advantages make NPs a suitable drug delivery system for treatment of wide variety of diseases, particularly in the management of cancer. Nanoparticles loaded with immunomodulatory agents have the ability to activate immune cells and modulate the tumor microenvironment to improve the antitumor immunity.[10] Brain tumor was the area of interest for many researchers who studied the role of NPs in the early detection and management of brain tumors.[11]

The term transdermal drug delivery system (TDDS) refers to a discrete dosage form which is applied directly to an intact skin layer to deliver the API payload to the systemic circulation.[12] The goals of TDDS development are to reduce the toxicity and increase the therapeutic effect of drugs by avoiding first-pass metabolism.[13] Therefore, drugs with poor bioavailability due to first-pass metabolism are good candidates for TDDS delivery. Transdermal drug delivery system allows for self-medication and termination of the drug input at any time by simply removing the formulation, and thus patient compliance can be more readily achieved. First-generation TDDS, which steady gained increasing clinical use in the past, has been utilized in the delivery of small, lipophilic, and low-dose drugs. Second-generation TDDS added more functionality by using chemical enhancers, nanocavities, ultrasound, and iontophoresis. Third generation TDDS has been used to specifically target the skins barrier layer of the stratum corneum (SC) by using thermal ablation and microneedle techniques.[14] Transdermal patches, successful tools in TDDS, are classified into 5 main categories: single-layer Drug-in-Adhesive system, multilayer Drug-in-Adhesive system, Reservoir, Matrix, and Vapor film.[15] In the first type, the adhesive layer containing the drug serves to attach the layers of the patch, attaches the patch to the skin, and is responsible for the drug release. This layer is enclosed by a temporary liner and a packing membrane. The multilayer Drug-in-Adhesive system is similar to the first type; however, the system contains immediate drug release layers and another layer for control release of the drug from a reservoir. In the third type, the reservoir, the layer that contains a drug solution or suspension, is surrounded by a rate-controlling polymeric membrane that enables the system to release the drug by a zero-order rate. The matrix-type system contains a drug layer in the form of a solution or suspension in a semisolid matrix. Finally, the vapor patches release their content of essential oils in an extended-release period up to 6 hours and are used for decongestion, sleep-aid, and to help in smoking cessation.

Dapoxetine (DPX), is a potent, short-acting selective serotonin reuptake inhibitor that is used as oral antidepressant medication.[16] Dapoxetine is currently licensed in more than 50 countries worldwide for the treatment of premature ejaculation (PE).[17] Dapoxetine is soluble in acidic medium but practically insoluble at a neutral pH of body fluids thus exhibits a pH-dependent solubility.[18] The mechanism of action of DPX in the treatment of PE is still unclear; however, it is presumed to work by blocking presynaptic membranes of 5-H transporters (ie, serotonin transporter) and as a consequence increases serotonin activity in the synaptic cleft. This central inhibition of the serotonin reuptake results in delayed ejaculation time and provides beneficial effects into PE.[19] Dapoxetine is rapidly absorbed after oral administration, reaches peak plasma level within 1 hour, and is rapidly eliminated from the body with a very short half-life of 1.2 hours.[20] Moreover, DPX is highly bound to plasma proteins (99%) and exhibits a volume of distribution of 2.1 L/kg.[21] The drug is extensively metabolized in the liver by cytochrome P450 isoforms and flavin-containing monooxygenase 1, the effect that results in the formation of an active metabolite, dapoxetine-N-oxide, and other numerous inactive metabolites. Therefore, due to the extensive first-pass metabolism, DPX shows a poor oral bioavailability of 42%.[18]

In this work, DPX-loaded chitosan (CS)-alginate (ALG) PNPs were prepared using the ionotropic gelation technique. The prepared PNPs were characterized for particle size, morphology using scanning electron microscope (SEM), and entrapment efficiency (EE). The optimized drug PNPs were incorporated into transdermal films that were prepared according to the solvent casting the method using different percent of surfactant of various hydrophilic–lipophilic balance (HLB). The prepared films were further characterized for cumulative percent of drug released and percent elongation. In addition, ex vivo permeation and transport of the PNPs across the skin layers were investigated.

Materials

Dapoxetine ((S)-N, N-dimethyl-3-(naphthalene-1-yloxy)-1-phenylpropane-1-amine hydrochloride) was a kind gift from Saudi Arabian Japanese (SAJA) Pharmaceuticals Company. Sodium tripolyphosphate (TPP), propylene glycol (PG), low molecular weight CS, tween 80, span 80, and formic acid were purchased from Sigma-Aldrich. Sodium ALG and calcium chloride ($CaCl_2$) were procured from VWR International Co, Ltd. Glacial acetic acid was purchased from Superchem Product Ltd. Acetonitrile, high-performance liquid chromatography (HPLC) grade, was obtained from Fisher Scientific Ltd. Hydroxypropyl methylcellulose (HPMC) Mwt 86 000 g/mol, viscosity 4000 cp, 2% solution, was procured from Acros Organics. All other chemicals and solvents were analytical grade.

Table 1. Composition and Characterization of Dapoxetine Nanoparticles Formulations Obtained from Box–Behnken Design.

				Y_1				Y_2	
Run	X_1 (%)	X_2 (%)	X_3 (%)	Observed (nm)	Predicted (nm)	PDI	Z potential (mV)	Observed (%)	Predicted (%)
F1	1:2	4:1	10:1	576.67 ± 50.65	545.46	0.161 ± 0.05	−5.35 ± 0.68	33.80 ± 3.36	29.45
F2	1:1	2:1	10:1	713.33 ± 68.07	735.38	0.203 ± 0.010	−3.85 ± 0.12	23.75 ± 2.88	26.89
F3	2:1	4:1	10:1	901.00 ± 63.27	897.71	0.631 ± 0.075	30.57 ± 1.75	23.65 ± 2.82	22.15
F4	1:2	4:1	5:1	488.67 ± 36.23	491.96	0.558 ± 0.025	−5.67 ± 1.93	13.17 ± 1.93	14.66
F5	2:1	4:1	5:1	783.34 ± 40.28	814.55	0.639 ± 0.09	19.83 ± 5.45	21.89 ± 2.08	26.23
F6	2:1	2:1	7.5:1	825.67 ± 51.00	806.92	0.429 ± 0.022	7.68 ± 1.13	29.83 ± 1.82	28.16
F7	1:1	6:1	10:1	775.00 ± 57.65	787.46	0.611 ± 0.036	14.07 ± 1.67	15.55 ± 1.63	18.25
F8	1:2	2:1	7.5:1	411.34 ± 40.25	420.51	0.449 ± 0.063	−6.76 ± 0.24	37.31 ± 2.36	38.51
F9	1:2	6:1	7.5:1	510.34 ± 40.50	529.089	0.262 ± 0.014	−3.88 ± 0.24	13.88 ± 1.81	15.53
F10	2:1	6:1	7.5:1	826.67 ± 77.16	817.50	0.505 ± 0.038	36.63 ± 1.01	31.32 ± 2.74	30.11
F11	1:1	6:1	5:1	748.67 ± 65.08	726.63	0.531 ± 0.026	25.53 ± 4.32	14.15 ± 0.9	11.00
F12	1:1	2:1	5:1	672.00 ± 60.51	659.54	0.275 ± 0.029	−2.41 ± 0.13	26.14 ± 2.60	23.43
F13	1:1	4:1	7.5:1	734.34 ± 67.36	741.23	0.512 ± 0.018	13.6 ± 0.17	23.23 ± 1.46	23.95
F14	1:1	4:1	7.5:1	751.00 ± 64.10	741.23	0.504 ± 0.052	12.93 ± 1.01	25.19 ± 2.01	23.95
F15	1:1	4:1	7.5:1	738.34 ± 61.50	741.23	0.469 ± 0.040	16.13 ± 1.32	23.42 ± 1.89	23.95

Abbreviations: X_1, chitosan to alginate ratio; X_2, chitosan to tripolyphosphate ratio and X_3, alginate to calcium chloride ratio; Y_1, particle size; Y_2, entrapment efficiency; PDI, polydispersity index.

Methods

Development of DPX CS-ALG PNPs

Box–Behnken experimental design. The effects of 3 different formulation factors affecting the particle size (Y_1) and the EE (Y_2) of DPX PNPs were studied using a 3-level, 3 factor Box–Behnken experimental design. The design was employed to statistically optimize the concentration of the studied polymers and the cross-linking agents. The design space included the effects of 3 variables, specifically the CS to ALG ratio (X_1), CS to TPP ratio (X_2), and ALG to $CaCl_2$ ratio (X_3). StatGraphics Plus software version 4 was used. The studied levels for the independent factors were 1:2 to 2:1, 2:1 to 6:1, and 5:1 to 10:1 for X_1, X_2, and X_3, respectively. The goal was to minimize Y_1 and maximize Y_2. The composition of 15 experimental runs, obtained from the design, is shown in Table 1.

Preparation of the PNPs. Polymeric NPs loaded with DPX were prepared according to the ionotropic gelation method utilizing different ratios of CS-ALG polymers and 2 different cross-linking agents. Briefly, 2 aqueous polymeric solutions of CS and ALG containing 0.25% were prepared by dissolving the calculated amount of each polymer in 5% (vol/vol) acetic acid solution and distilled water, respectively. Each polymeric solution was left on a magnetic stirrer overnight to allow complete dissolving of the polymer. According to the formulation composition illustrated in Table 1, the known weight of DPX was dissolved in the specified volume of CS, and the predetermined amount of $CaCl_2$ was added. The calculated amount of TPP was dissolved in the specified volume of ALG solution. The prepared ALG-TPP solution was subsequently added dropwise to the medicated CS-$CaCl_2$ solution over a high-speed Homogenizer, Ultra Turrax, IKA, T25, digital Homogenizer at 20 000 rpm for 15 minutes. The obtained suspension containing DPX PNPs was filled in Eppendorf tubes and centrifuged at 15 000 rpm for 60 minutes at 5 °C using Sigma Laboratory centrifuge, 3K30. The precipitated PNPs were separated, washed, subjected for freezing at −80 °C and finally were lyophilized using Christ Alpha 1-2 LD Plus lyophilizer to obtain a dried powder of DPX PNPs.

Characterization of the Formulations

Particle size distribution and Z potential. The average particle size, polydispersity index (PDI), and Z potential values for the 15 DPX PNPs formulations were measured by dynamic light scattering using a Malvern Zetasizer Nano Z5P, Malvern Panalytical Ltd. All measurements were repeated in triplicate.

Entrapment efficiency. The percent of DPX that was successfully entrapped into the prepared PNPs was estimated indirectly. Briefly, the obtained PNPs dispersions were subjected to centrifugation at 15 000 rpm for 60 minutes at 5 °C using a cooling centrifuge from Sigma laboratory, 3K30. The supernatant containing the free drug was collected, filtered using an Acrodisc syringe filter of 0.2 μm, and analyzed for DPX using HPLC as reported in the literature.[22] An Agilent 1200 series that is equipped with a temperature-controlled autosampler was used. The mobile phase composed of a mixture of acetonitrile and 0.1% formic acid (80:20, vol/vol). The flow rate was adjusted at 1.5 mL/min, the absorbance was determined at 291 nm, and the injection volume was 0.5 μL.

EE of DPX in the prepared PNPs formulations was calculated using the following equation:

$$EE\ (\%) = \frac{\text{Theoretical total DPX Concentration} - \text{Calculated free DPX in the supernatant}}{\text{Theoretical total DPX Concentration}} \times 100.$$

Table 2. Composition and Characterization of Dapoxetine Transdermal Film Formulations Obtained From 3-Level Factorial Design.[a]

					Y_1` (%)		Y_2` (%)	
Run	X_1` (HLB)	X_2` (%)	Drug content (mg)	Thickness (mm)	Observed	Predicted	Observed	Predicted
A1	4.3	0.2	1.189 ± 0.111	0.243 ± 0.041	83.000 ± 7.056	79.139	25	25.417
A2	4.3	0.6	1.215 ± 0.091	0.264 ± 0.013	69.889 ± 4.998	75.022	37.5	34.167
A3	15.0	0.6	1.191 ± 0.114	0.281 ± 0.017	62.087 ± 6.719	56.989	30	35.0
A4	4.3	1.0	1.201 ± 0.121	0.259 ± 0.029	75.495 ± 7.049	74.039	50	52.917
A5	9.65	1.0	1.262 ± 0.113	0.298 ± 0.022	49.811 ± 3.201	47.356	50	48.333
A6	15.0	1.0	1.255 ± 0.124	0.283 ± 0.027	37.922 ± 2.507	41.706	42.5	41.25
A7	9.65	0.2	1.198 ± 0.102	0.242 ± 0.014	64.266 ± 5.117	66.756	30	33.333
A8	9.65	0.6	1.251 ± 0.120	0.274 ± 0.021	55.667 ± 4.807	55.489	37.5	35.833
A9	15.0	0.2	1.193 ± 0.122	0.235 ± 0.022	74.056 ± 6.303	75.406	42.5	38.75

Abbreviation: X_1`, surfactant hydrophilic–lipophilic balance (HLB); $X_2$`, surfactant percent; Y_1`, cumulative percent of drug released; $Y_2$`, elongation percent.
[a]A drug concentration of 1.26 mg was loaded into each film of 1.76 cm2.

Box–Behnken Experimental Design Statistical Analysis

The data obtained for Y_1 and Y_2 were introduced into the response column of the StatGraphics software and statistically analyzed. A *P* value less than .05 was considered significant. The optimum desirability was identified, and an optimized formulation was proposed.

Preparation and Characterization of the Optimized PNPs Formulation

The optimized DPX loaded PNPs formulation that contains the proposed values of X_1, X_2, and X_3 were prepared and characterized for Y_1 and Y_2, as previously mentioned. The differences between the predicted and observed values were calculated.

Dapoxetine content in the prepared optimized PNPs was determined by accurately weighing a known weight of the dried PNPs formulation and dispersing in a specified volume of 10% (vol/vol) acetic acid solution. The mixture was homogenized and kept in shaking water bath, GFL GrP for 48 hours. The obtained dispersion was filtered using a 0.2-μm membrane filter, and DPX content was estimated using HPLC method previously described.

The surface morphology of the optimized PNPs formulation was visualized using a SEM, Philips XL30. The freeze-dried optimized PNPs formulation was fixed on a carbon tape and was sputter-coated with gold before investigation. The accelerating voltage was set at 20 kV.

Solid-State Physicochemical Characterization

Differential scanning calorimetry. The thermal behavior of pure DPX, CS, ALG, a physical mixture of DPX, CS, ALG, and the dried optimized PNPs was investigated using a Shimadzu DSC TA-50 ESI differential scanning calorimetry (DSC) apparatus. About 2 mg of each sample was placed in an aluminum crucible under an atmosphere of nitrogen and heated at a rate of 10 °C/min from 25 °C to 300 °C.

Fourier-transform infrared spectroscopy. The IR spectra of the same samples, studied in the above section, were recorded in range 4000 to 400 cm^{-1} using a Nicolet iS10 Fourier-transform infrared spectroscopy (FT-IR) spectrometer, Thermo Scientific, Inc.

X-ray powder diffraction (XRD). To examine the crystalline state of DPX in the developed optimized drug PNPs, samples of the optimized dried PNPs formulation and pure DPX powder were examined using a D/max 2500; Rigaku, Powder X-ray diffractometer. The diffraction patterns of the samples were recorded at a scan speed of 0.5 °C/min.

Development of Transdermal Films Loaded With DPX PNPs

Three-level factorial design. A 3^2 factorial design has been implemented to study the effect of 2 independent factors, each at 3 levels, on the development of an optimized transdermal film characterized by good elongation percent and maximum cumulative percentage of drug released. The design space includes studying the effect of 2 independent variables, namely; surfactant HLB (X_1`) and the surfactant percent ($X_2$`) on the cumulative percent of drug released (Y_1`) and the percent elongation ($Y_2$`) of the prepared transdermal films. The studied levels for the independent variables were 4.3 to 15 HLB, and 0.2% to 1% (weigh/vol) for X_1` and $X_2$`, respectively. Nine formations have been proposed. The order of the experiments has been fully randomized to provide protection against the effects of lurking variables. The composition of these formulations is demonstrated in Table 2.

Preparation of transdermal films loaded with DPX PNPs. Transdermal films loaded with the optimized DPX PNPs were prepared according to the solvent casting technique.[23,24] A known weight of the PNPs equivalent to 46 mg DPX and a specified quantity of HPMC, used as a film-forming substance, were added to distilled water containing the calculated amount of the nonionic surfactant over a magnetic stirrer at 1000 rpm. Propylene glycol (1%) was added as a plasticizer. Stirring was

continued until a homogenous mixture was obtained. The mixture was left overnight in the refrigerator at 5 °C to allow formation of a clear solution free from air bubbles. The polymeric drug-loaded solution was poured into a glass Petri dish of 9 cm in diameter. A silicone-coated liner (3M, ScotchpakTM, St Paul, MO) was used to cover the dish that was kept in an oven at 45 °C until the solvent was completely evaporated and a dried semi-solid formulation was obtained. The prepared films were subsequently cut into pieces of 1.76 cm^2 areas and stored in a tightly closed desiccator maintained at room temperature. A drug concentration of 1.26 mg was loaded into each film of 1.76 cm2.

Characterization of the Prepared Films

Drug content. Triplicate samples of each film (1.76 cm2) were separately transferred into a graduated glass stopper flask containing a specific volume of 10% (vol/vol) acetic acid solution. The flasks were kept at room temperature for 72 hours in a shaking water bath GFL GrP. The obtained solutions were filtered through a 0.2-µm membrane filter, and the drug content was estimated using HPLC method mentioned above.

Thickness. The thickness of the prepared films was measured at different points using a digital micrometer Mitutoyo Co, and the average thickness (n = 3) was determined.

Percent elongation. To identify the maximum elongation of the prepared films, relative to the original length, upon application of a specified force or weight, the percent elongation was determined. This character was evaluated using an elongation mechanical test apparatus that was designed in our laboratory and according to the procedure previously published.[25] Small rectangular strips of 4-cm-long and 1-cm-width were cut. Each piece was placed between the upper and lower clamp jaws in which 2-cm-long was maintained between the 2 jaws. A constant weight was fixed to the lower clamp jaw. After 5 minutes, the increase in length was recorded, and the percent elongation was calculated using the following equation:

$$\text{Elongation}(\%) = [(L_f - L_0)/(L_0)] \times 100,$$

where L_0 is the initial length of each film and L_f is the final length of each film.

Ex Vivo Skin Permeation Study

The *ex vivo* skin permeation of DPX PNPs from the prepared transdermal films was evaluated using Franz diffusion cell (Microette Plus; Hanson research). The study was conducted in accordance with the role Declaration of Helsinki and the guiding principles in the care and use of laboratory animals (DHEW publication NIH 80-23). The handling of the experimental animal in this study has received prior approval by the Faculty of Pharmacy, King Abdulaziz University Institutional Board for Preclinical and Clinical Research Experiment, who verify the laboratory animal care (approval number: 111439). Male Wistar rats (200-250 g) were sacrificed by cervical dislocation. The skin abdomen was shaved, and the full skin thickness was cut out surgically, washed with normal saline, and divided into small uniform circular pieces of 3 cm diameter. The prepared skin pieces were placed between the receptor and the donor cells of the diffusion apparatus so that the skin dermis was in contact with the receptor compartment. The prepared films were applied to the donor compartment. Phosphate buffer saline of pH 7.4 was used as a receptor medium that was maintained at 37 C. A constant stirring speed of 400 rpm was kept during the experiment. Aliquots from the receptor compartment were withdrawn at 0.5, 1, 2, 4, 6, 8, 10, 12, 18, and 24 hours. The concentration of DPX in the collected samples was analyzed by HPLC. The condition of the experiment was adjusted to achieve a sink condition. Dapoxetine steady flux (*Jss*) was calculated from the slope of the gradient portion of the linear curve obtained following plot of the cumulative DPX permeated per unit area against time. Dapoxetine permeability coefficient (P) was determined using the equation:

$$P = Jss/C_o$$

Where C_o is the initial DPX concentration applied in the donor compartment. Dapoxetine diffusion coefficient (D) was calculated by representing the cumulative amount of DPX permeated against the square root of time and applying the following equation:

$$D = (\text{slope}/C_o)^2 \times \pi.$$

Three-Level Factorial Design Statistical Analysis

The obtained data for Y_1 and Y_2 were introduced into the StatGraphics software and analyzed to identify the statistical significance between the independent variables and the studied responses. Statistical analysis of the data was considered to be significant at P value < .05. The optimum desirability was calculated, and an optimized formulation was proposed. This formulation was prepared and characterized for Y_1 and Y_2 as previously mentioned, and differences between the predicted and observed values were calculated. A pure drug-loaded transdermal film, containing the optimized level of X_1 and X_2, was also prepared and characterized, and the cumulative DPX released was compared to that of the optimized formulation containing DPX PNPs.

Fluorescence Laser Microscopy Analysis

Transport of the PNPs across the skin layers was studied using a Zeiss Axio Observer D1 Inverted DIC Fluorescence Microscope (Carl Zeiss AG). Polymeric NPs loaded with fluorescence isothiocyanate (FITC), instead of DPX, were prepared and loaded into the optimized film as previously described. A pure FITC loaded film was also prepared as a control. Both films were applied to the excised skin that was mounted on the Franz diffusion cell apparatus. The skin was removed after 1, 2, and 4 hours. The collected skin samples were kept in formalin. A longitudinal section in each sample using microtome blades

Table 3. Analysis of Variance for the Nanoparticles Size and Entrapment Efficiency.

	Y_1			Y_2		
Formulation	Estimated effect	F-ratio	*P* value	Estimated effect	F-ratio	*P* value
X_1	337.415	266.40	.00001[a]	2.13	0.52	.5034
X_2	59.5825	8.31	.0345[a]	−10.53	12.69	.0162[a]
X_3	68.3325	10.93	.0213[a]	5.355	3.28	.1298
X_1X_1	−137.554	20.43	.0063[a]	7.36583	2.87	.1512
X_1X_2	−49.0	2.81	.1546	12.455	8.88	.0308[a]
X_1X_3	14.83	0.26	.6335	−9.435	5.09	.0736
X_2X_2	−57.8892	3.62	.1155	0.905833	0.04	.8433
X_2X_3	−7.505	0.07	.8076	1.895	0.21	.6693
X_3X_3	29.9408	0.97	.3703	−9.01417	4.29	.0930
*R*2		98.4313%			88.4982%	
Adj-*R*2		95.6077%			67.795%	
SEE		29.2355			4.18009	
MAE		14.2244			2.10511	

Abbreviations: Adj-R^2, adjusted R^2; MAE, mean absolute error; R^2, R-squared; SEE, standard error of estimate; X_1; CS: ALG, X_2; CS: TPP, X_3; ALG: $CaCl_2$, X_1X_2, X_1X_3, and X_2X_3, are the interaction terms of factors; X_1X_1, X_2X_2, and X_3X_3 are the quadratic terms of factors; Y_1, particle size; Y_2, entrapment efficiency.
[a]Significant effect of factors on individual responses, *P* value < .05.

was performed from paraffin wax skin samples. Images were taken using 470/40 nm excitation, 495 beam splitter, and 525/50 nm emission.

Results and Discussion

Preparation and Characterization of DPX PNPs

In this study, DPX PNPs have been developed by the ionotropic gelation technique utilizing the double-crossing technique. The prepared PNPs were separated by centrifugation, washed, freeze-dried, and finally characterized for size, EE, PDI, and Z potential. Table 1 illustrates the obtained results of the PNPs characterization for the 15 Box–Behnken formulations. Results revealed that the particle size of the DPX PNPs was in the range of 411.33 ± 40.25 to 901 ± 63.27 nm, and the EE was between 13.17 ± 1.93 and 37.31% ± 2.36%. The values of the PDI were in the range of 0.161 ± 0.05 to 0.639 ± 0.09. The obtained results for the PDI indicate homogeneity and acceptable size distribution of the prepared PNPs. Danaei et al reported that PDI values smaller than 0.05 are mainly observing with highly monodispersed systems, while PDI values greater than 0.7 indicate that the prepared sample has a very broad particle size distribution.[26] Accordingly, the prepared PNPs displayed acceptable homogeneity. Z potential, which is a key indicator of NPs stability,[27] was affected by the formulation composition. Formulation with high ALG content (1:2 CS to ALG ratio), namely F1, F4, F8, and F9 showed negative polarity, while those with high CS content (2:1 CS to ALG ratio), namely F3, F5, F6, and F10 demonstrated positive polarity. Formulations with an equal ratio of both polymers were highly affected by the CS to TPP ratio (X_2) and ALG to $CaCl_2$ ratio (X_3). At a CS to ALG ratio (X_1) of 1:1 and ALG to $CaCl_2$ ratio (X_3) of 10:1, formulation with low TPP, namely F7, exhibited positive polarity, while that with high TPP, namely F2, illustrated negative polarity. Also, at a CS to ALG ratio (X_1) of 1:1 and ALG to $CaCl_2$ ratio (X_3) of 5:1, formulation with low TPP, namely F11, showed positive polarity, while that with high TPP, namely F12, exemplified negative polarity. Finally, at a CS to ALG ratio (X_1) of 1:1 and ALG to $CaCl_2$ ratio (X_3) of 7.5:1, formulations F13, F14, and F15 with relatively high CS, and low TPP (4:1) showed positive polarity.

Optimization of the DPX PNPs

The observed values for the particle size and EE, illustrated in Table 1, were statistically analyzed by multiple regression analysis and 2-way analysis of variance (ANOVA) to indicate the effect of X_1, X_2, and X_3, on Y_1 and Y_2. Table 3 demonstrates the values for the estimated effect, F-ratios, and the associated *P* values. A positive value for the estimated effect is an indication of a synergistic effect of this independent variable on the studied response, while a negative value is a sign of an antagonistic effect. Moreover, the actual and expected variations in the variable average are compared, and the F-ratio is calculated. A value of F-ratio greater than 1 indicates the presence of a location effect, and therefore, the *P* value should be reported to specify the significance level. The studied factor is considered significant if a *P* value less than .05 is obtained. The polynomial equations of the fit model were found to be:

$$Y_1 = 3901.57 + 36.415 \times X_1 + 68.590 \times X_2 - 171.002 \times X_3 - 0.248 \times X_1^2 - 0.154 \times X_1X_2 + 0.118 \times X_1X_3 - 0.319 \times X_2^2 - 0.104 \times X_2X_3 + 1.045 \times X_3^2 \quad \text{(Equation1)}$$

$$Y_2 = -2326.4 + 2.263 \times X_1 - 5.568 \times X_2 + 57.264 \times X_3 + 0.013 \times X_1^2 + 0.039 \times X_1X_2 - 0.075 \times X_1X_3 + 0.005 \times X_2^2 + 0.026 \times X_2X_3 - 0.315 \times X_3 \quad \text{(Equation2)}$$

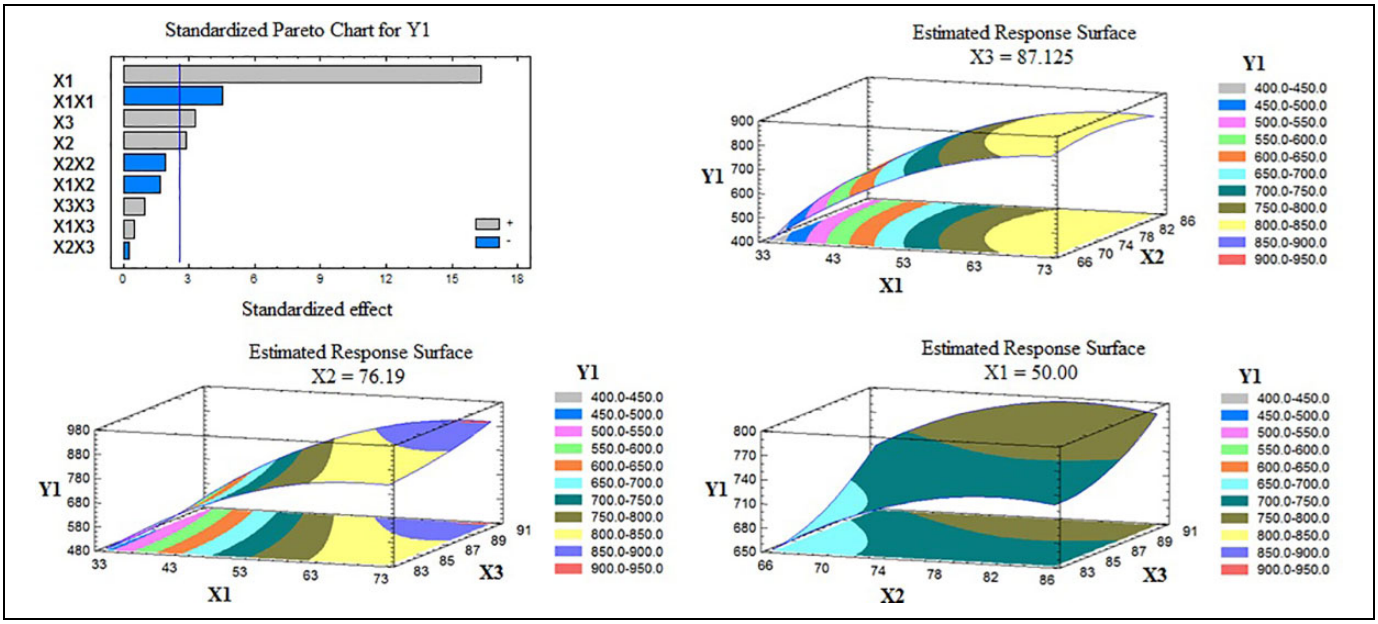

Figure 1. Standardized Pareto chart and estimated response surface plots for the effect of the studied variables on particle size.

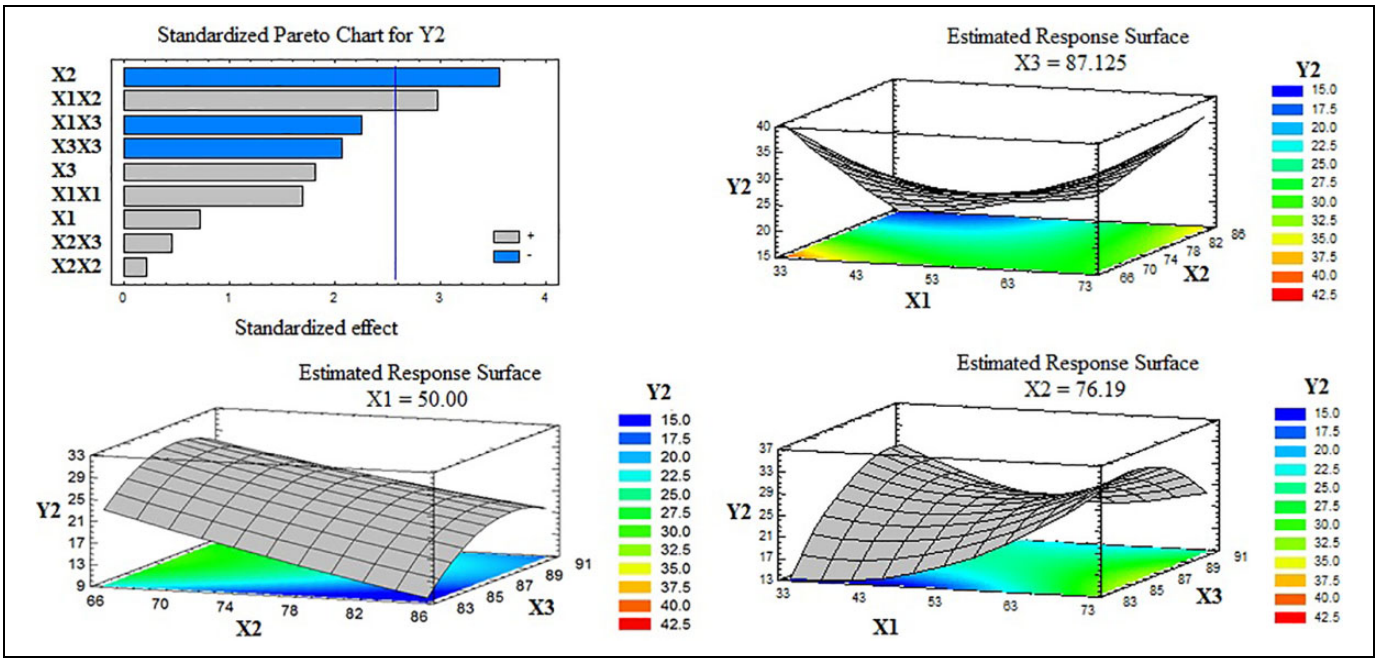

Figure 2. Standardized Pareto chart and estimated response surface plots for the effect of the studied variables on entrapment efficiency.

Analysis of variance revealed a marked significant effect of X_1, X_2, X_3, and X_1X_1 on Y_1 at a P values of .00001, .0345, .0213, and .0063, respectively. The effects of the studied factors on Y_1 are illustrated in the Pareto chart and 3-dimensional surface plots shown in Figure 1. A synergistic effect was observed for X_1, X_2, and X_3 on Y_1. As the ratio of CS:ALG (X_1) increased from 1:2 to 2:1, the average particle size was increased, the effect that could be attributed to the formation of multiple coating layers of CS by precipitation of the polymer on the PNPs surface.[25] Similar results were also reported by Bhunchu et al, during the development of CS-ALG PNPs loaded with curcumin.[28] The authors mentioned that the particle size of the prepared PNPs was significantly affected by CS:ALG ratios and large size particles were observed at higher CS ratio. The increase in particle size and PDI obtained upon increasing CS:ALG could also be explained by the particle aggregation and compact membrane formation of CS on the surface of PNPs.[28]

Pent sodium TPP is a nontoxic, negatively charged polyanionic phosphate polymer. It is commonly used as a cross-linking agent during the preparation of CS-based PNPs.[29]

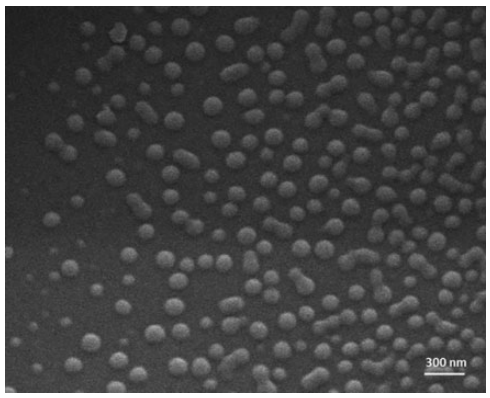

Figure 3. Scanning electron microscope imaging for the optimized dapoxetine polymeric nanoparticles.

Chitosan:TPP mass ratio (X_2) also significantly affected the size of the developed PNPs. Previous studies indicated that there is a direct correlation between decreasing the CS: TPP mass ratio and producing smaller PNPs.[29] Better cross-linking and smaller PNPs are achieved at low CS:TPP mass ratio. At high CS-TPP mass ratio, the available TPP quantity is small, and so TPP might not be enough to produce inter- and intramolecular cross-link with CS to form small PNPs. The same approach could be applied to the ALG:$CaCl_2$ ratio (X_3). $CaCl_2$ binds with the guluronic acid blocks of the ALG macromolecule. Insufficient interaction may occur at low $CaCl_2$ (high ALG:$CaCl_2$ mass ratio), the effect that causes insufficient gelation and decrease microparticles or NPs formation.[30]

Based on the ANOVA for the effect of the studied variables on Y_2, it was indicated that the interaction effects of X_1X_2 had a main synergistic effect on Y_2 at a P value of .0308, while X_2 was antagonistically affecting Y_2 at a P value of .0162. Stoica and Ion reported an antagonistic effect of CS:TPP mass ratio on the drug EE during their preparation of CS-TP PNPs loaded with natural extract of rose hips.[31] The effect of the studied factors on Y_2 is demonstrated in the Pareto chart and 3-dimensional surface plots that are shown in Figure 2.

Preparation and Characterization of an Optimized PNPs Formulation

Based on the desirability function approach, numerical optimization was employed (ie, based on the desirability function approach) to predict the optimum condition used to develop an optimized DPX PNPs formulation with minimum particle size and maximum EE. The optimum levels for X_1, X_2, and X_3 were 1:2, 2:1, and 7.5:1, respectively. An optimized formulation containing the abovementioned levels was prepared and characterized. The observed values for Y_1 and Y_2 were 415.943 nm and 37.31%, respectively.

A surface study of the optimized DPX PNPs formulation using SEM was performed, and the prepared optimized PNPs displayed approximately uniform spherical shape and size distribution, as illustrated in Figure 3.

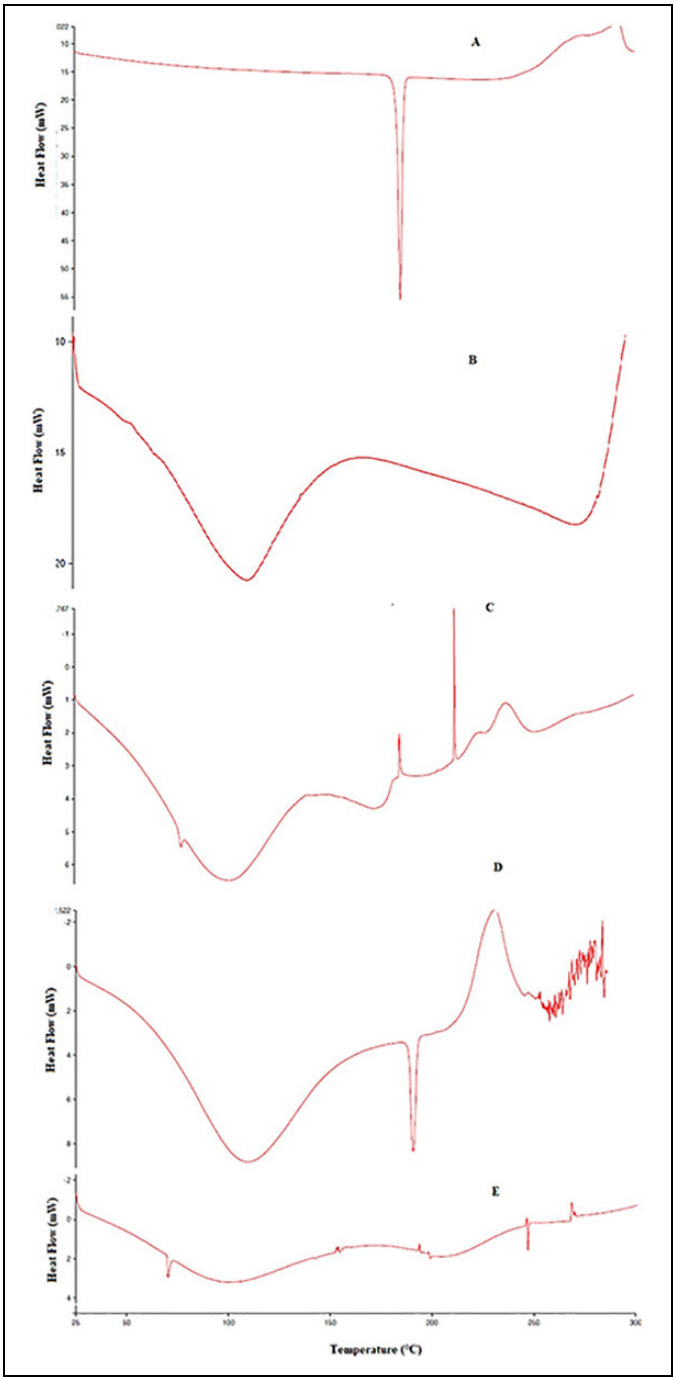

Figure 4. Differential scanning calorimetry thermogram of dapoxetine (A), chitosan (B), alginate (C), drug-polymeric physical mixture, (D) and the optimized drug nanoparticles formulation (E).

Compatibility Study

The DSC thermogram of pure DPX demonstrated a strong sharp endothermic peak approximately at 185.15 °C (Figure 4), corresponding to the drug melting point.[32] The thermogram of the physical mixture (DPX-CS-ALG) displayed smaller changes in the DPX melting point, where the endothermic peak was observed at 190.92 °C, which indicates no possible interaction between the drug and the studied polymers. The DSC thermogram of the

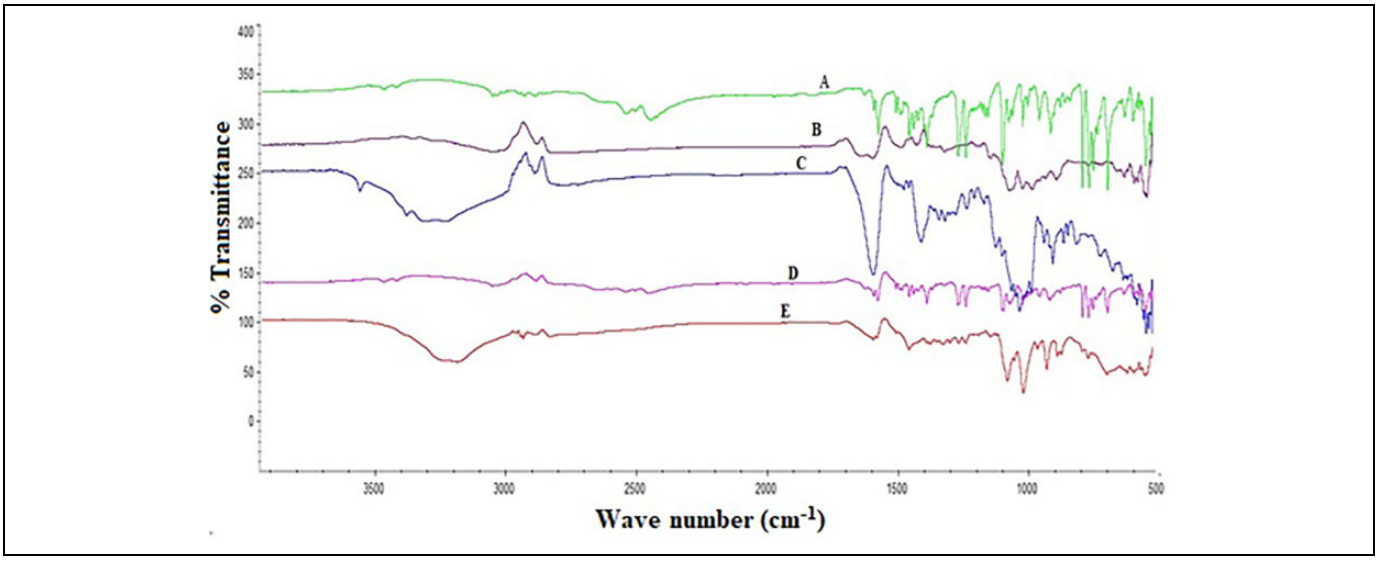

Figure 5. Fourier transform infrared spectroscopy spectra of dapoxetine (A), chitosan (B), alginate (C), drug-polymeric physical mixture, (D) and the optimized drug nanoparticles formulation (E).

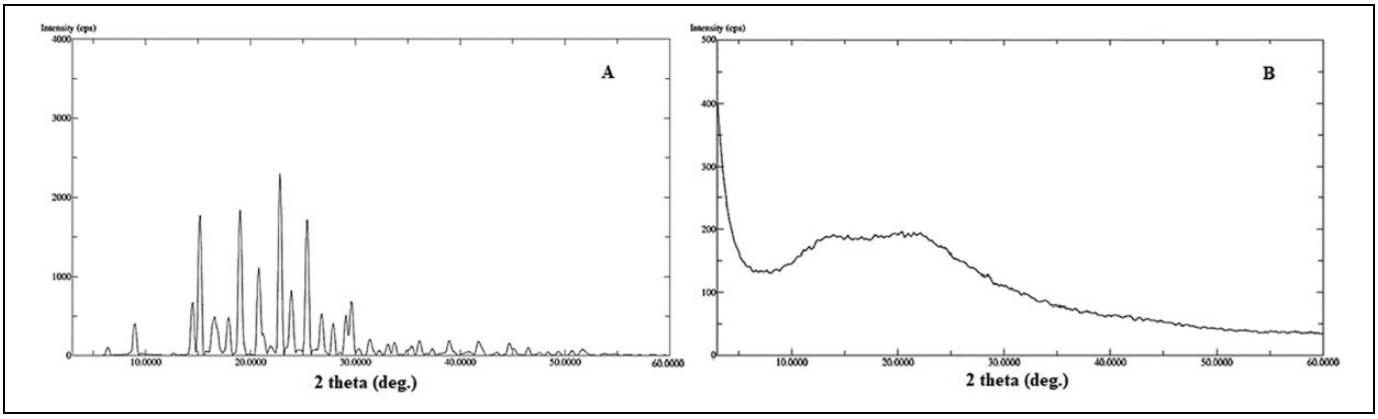

Figure 6. X-ray powder diffraction patterns of pure DPX (A) and the optimized DPX nanoparticles (B). DPX indicates dapoxetine.

optimized DPX PNPs showed a completely different pattern. The absence of the DPX peak might indicate that the drug was fully entrapped in the polymeric matrix. The absence of the drug peak could also be attributed to the possibility of drug crystalline change as previously reported by Fouad et al during the development of a similar DPX nanocarrier system.[33] Crcarevska et al stated similar findings for CS-coated Ca-ALG microparticles loaded with budesonide, where they attributed the absence of budesonide endothermic peak to the complete drug entrapment in the polymer matrix as well as the drug crystallinity lowering. However, additional X-ray diffraction study is needed to better understand the absence of such peaks, as stated by the authors.[34]

The FT-IR spectra of pure DPX (Figure 5) illustrated characteristic peaks at 3050, 1583, and 1456 cm^{-1} corresponding to C-H stretching, C = O, and CH_3, respectively. The C = C stretching of the CS aromatic ring was detected at 1600 cm^{-1}, while the polymer ether functional group (O-R) was recorded approximately at 1100 cm^{-1}.[35] Moreover, the CS spectra showed a broadband in the range of 3300 to 2900 cm^{-1} corresponded to the amine and hydroxyl groups. A peak at 2876 cm^{-1} is attributed to −OH stretching; a characteristic band of the carbonyl (C = O) stretching of the secondary amide was detected at 1655 cm^{-1}, and the bending vibrations of the N-H (N-acetylated residues, amide II band) observed at 1599 cm^{-1}.[36] Other peaks at 1423 and 1381 cm^{-1} that belong to the N-H stretching of the amide and ether, respectively, were also detected. In the FT-IR spectrum of ALG, bands around 1030 cm^{-1} corresponding to C-O-C stretching are assigned to the sodium ALG saccharide structure. Also, bands detected in 1617, and 1417 cm^{-1} are attributed to asymmetric and symmetric stretching peaks of carboxylate salt groups.[37] No significant shifting in the DPX characteristic peaks was noticed upon the physical mixing of the drug with CS and ALG, while in the spectrum of the optimized DPX PNPs, a complete shift was noticed in the asymmetrical and the symmetrical stretching of the ALG carboxylic groups. Similarly, the CS N-H group, corresponding to N-acetylated residues of the amide and the stretching vibration of the CS -OH and $-NH_2$, was also shifted

and become broader. These changes indicate that the ALG carboxylic groups were associated with the CS ammonium groups, and both $CaCl_2$ and TPP interacted electrostatically with both polymers to form the polyelectrolyte complex.

The XRD was studied to evaluate the crystalline characteristics of the pure DPX and the optimized DPX PNPs formulation. The pattern of the pure drug, demonstrated in Figure 6 revealed numerous distinctive crystalline peaks particularly at 2θ of 22.80°, 19.00°, and 15.20°. On the other hand, the diffraction pattern of the optimized DPX PNPs showed a completely different pattern with an absence of the drug characteristic peaks. Accordingly, a change in the drug state from the crystalline to the amorphous might have occurred.

Preparation and Characterization of DPX Transdermal Films

A 3-level factorial design was employed to develop DPX transdermal films utilizing the solvent casting technique. Hydroxypropyl methylcellulose (2% weight/vol) and PG (1% vol/vol) were used as a film-forming polymer and a plasticizer, respectively. Additionally, the nonionic surfactants, tween 80 and span 80, were added as permeation enhancers.

The prepared DPX films were evaluated for the content uniformity, thickness, cumulative percent of drug released, and elongation percent. The obtained results for these parameters are shown in Table 2. Good content uniformity of the drug (95.01%-100.16%) was observed for the prepared films. Thickness was in the range 0.235 ± 0.022 to 0.298 ± 0.022 mm, and the elongation percent was ranged from 25% to 50%.

Ex vivo skin permeation study was carried out across the abdominal skin of male Wistar rats, and the drug release profile from the prepared DPX transdermal films is illustrated in Figure 7. The profiles of DPX permeation exhibited a sustained drug release pattern. The cumulative DPX released percent was 49.811% ± 3.201% to 83% ± 11.056%, as demonstrated in Table 2. The steady-state flux (J_{SS}), the P, and the D were estimated, and the obtained values for these permeation parameters are listed in Table 4.

*Effect of independent variables on the cumulative drug released (Y_1`).* The effect of the surfactant HLB ($X_1$`) and surfactant percent (X_2`) on the cumulative drug release ($Y_1$`) and elongation percent (Y_2`) was studied, and the observed and predicted values are illustrated in Table 2. Statistical analysis of the cumulative percent of drug release ($Y_1$`) data was performed by multiple regression analysis and 2-way ANOVA using StatGrafics software. The obtained values of the estimated effects, the F ratios, and *P* values for each response are displayed in Table 5. The equation of the model was found to be:

$$Y_1` = 104.698 - 6.77202 \times X_1` + 3.75818 \times X_2` + 0.367427 \times X_1`^2 - 3.34112 \times X_1`X_2` + 9.79167 \times X_2`^2. \quad \text{(Equation3)}$$

It was noticed that the surfactant HLB (X_1`) and surfactant percent ($X_2$`) were significantly affecting the cumulative percent of DPX released after 24 hours at a *P* value of .0310 and .0256, respectively. The Pareto chart, illustrated in Figure 8, confirmed this finding where both X_1` and $X_2$` showed

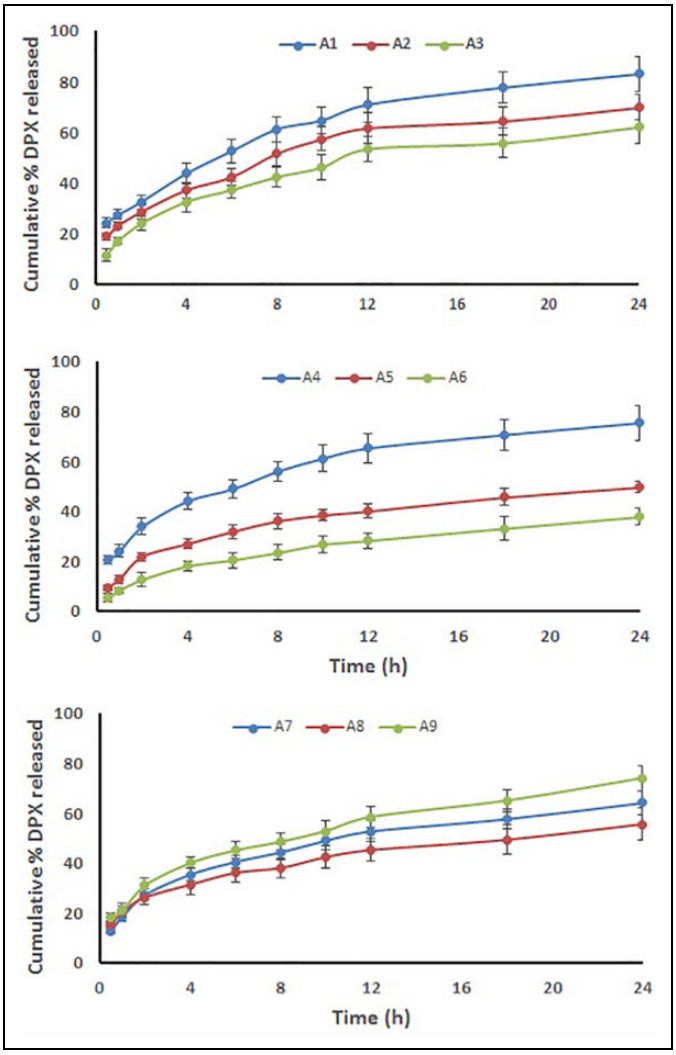

Figure 7. Ex vivo skin permeation study of dapoxetine from the prepared transdermal films.

Table 4. Ex Vivo Permeation Parameters of DPX From the Prepared Transdermal Films Loaded With the Optimized DPX PNPs.

Run	*Jss* (μg/cm²·min)	P × 10^{-4} (cm/min)	D × 10^{-4} (cm/min)
A1	0.591	4.691	1.124
A2	0.825	6.551	2. 136
A3	0.391	3.101	4.832
A4	0.429	3.404	5.779
A5	0.305	2.423	2.991
A6	0.368	2.924	4.229
A7	0.366	2.904	4.229
A8	0.378	3.002	4.526
A9	0.3183	2.526	3.209

Abbreviations: D, diffusion coefficient; DPX, dapoxetine; *Jss*, steady state flux; P, permeability coefficient; PNPs, polymeric nanoparticles.

Table 5. Estimated Effects of Factors, F-Ratio, and Associated *P* Value for DPX Transdermal Film Formulations Cumulative Drug Release and Elongation Percent.

	Y_1`			Y_2`		
Formulation	Estimated effect	F ratio	*P* value	Estimated effect	F ratio	*P* value
X_1`	−18.0333	14.80	.0310[a]	0.833333	0.04	.8533
X_2`	−19.4	17.13	.0256[a]	15.0	13.14	.0361[a]
X_1X_1`	21.0333	6.71	.0810	−2.5	0.12	.7503
X_1X_2`	−14.3	6.21	.0884	−12.5	6.08	.0904
X_2X_2`	3.13333	0.15	.7253	10.0	1.95	.2574

Abbreviations: DPX, dapoxetine; X_1`; surfactant HLB, $X_2$`; surfactant percent, X_1`$X_2$`; the interaction terms between the factors; X_1`$X_1$`and X_2`$X_2$`, the quadratic terms of the factors; Y_1`, the cumulative drug release; $Y_2$`, elongation percent.
[a]Significant effect of factors on individual responses, *P* value < .05.

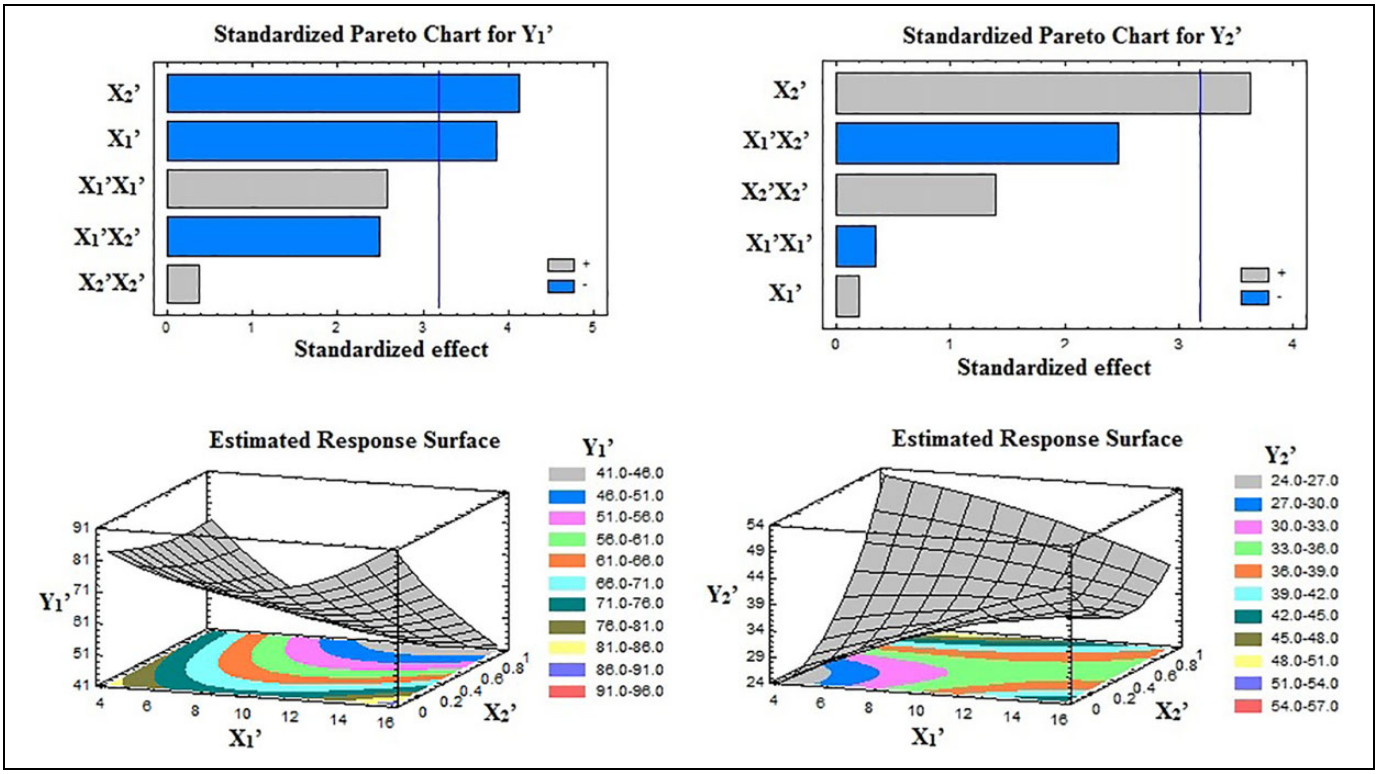

Figure 8. Standardized Pareto chart and estimated response surface plot for the effect of the studied variables on cumulative drug released and percent elongation.

an antagonistic effect on Y_1`. To indicate the effects of the studied variables on $Y_1$`, a response surface plot was constructed and is also illustrated in the same figure.

Recently, surfactants have been incorporated in a transdermal delivery system as a penetration enhancer to improve the drug skin permeation by disrupting the barrier function of the subcutaneous layer.[38] A wide range of surfactant HLB (4.3-15) was studied to investigate the impact of their hydro/lipophilicity on the drug release. Enhanced cumulative percent of drug release was achieved at a low surfactant HLB of 4.3, a value corresponding to a lipophilic surfactant property. This finding could be linked to the direct interaction between the predominantly lipophilic surfactant molecules and the phospholipid skin subcutaneous structures as well as to the increase in the lipid fluidity within the SC which facilitates the drug diffusion across the skin subcutaneous barrier structure.[39] It has been previously mentioned that the process of surfactant molecule penetration into the skin lipid lamellae of the SC is effectively dependent on the solubility and partitioning behavior of surfactant.[40] Wu et al reported that the permeation of inulin through the skin was highly dependent on the surfactant HLB value and stated higher inulin permeation at lower HLB.[41] Moreover, Cho et al concluded that the enhancement of the retinol permeation through the skin layer was also significantly

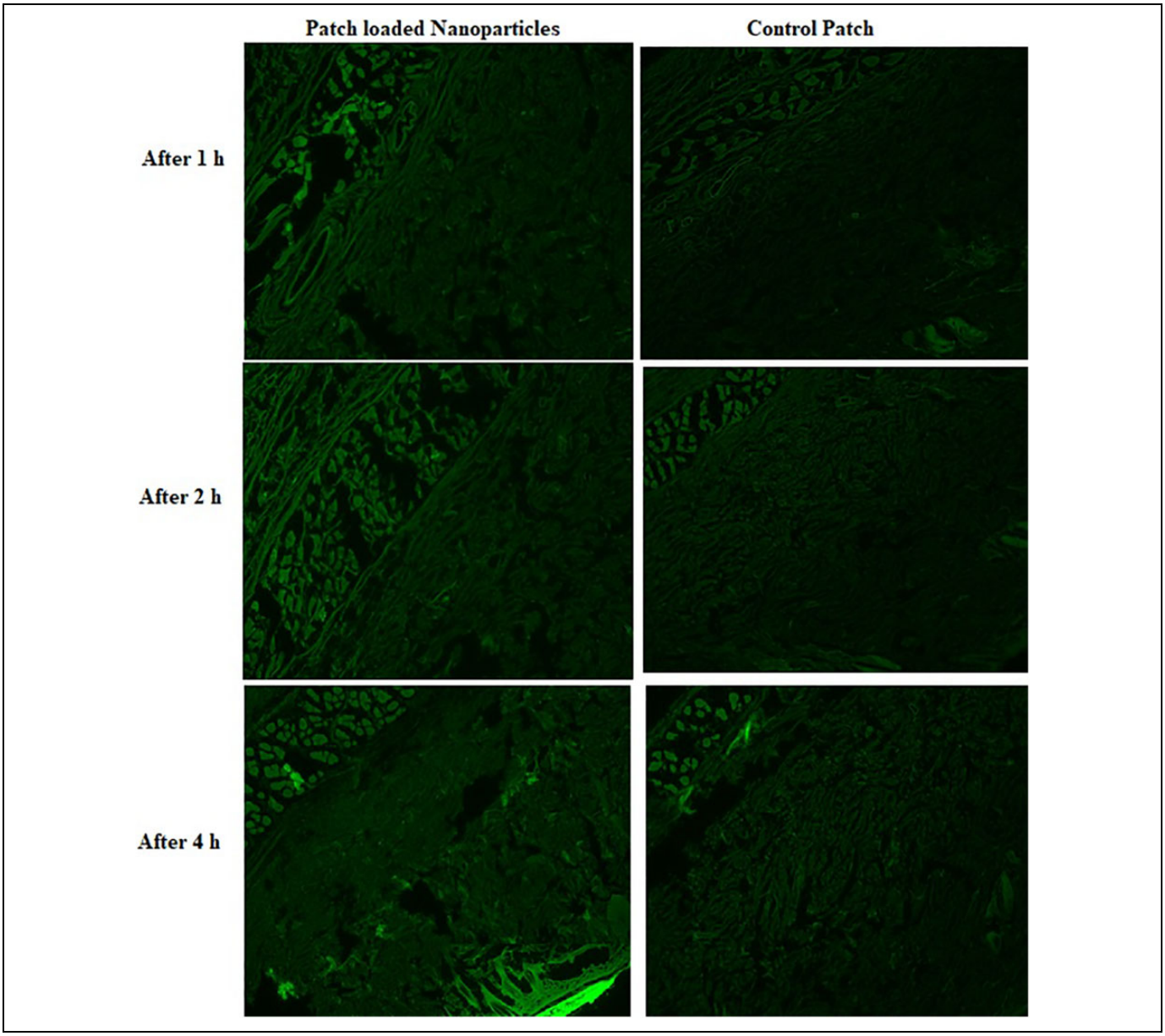

Figure 9. Fluorescence laser microscope images in rat skin layers following transdermal application of fluorescence-labeled polymeric nanoparticle films and films loaded pure fluorescein isothiocyanate (control) after 1, 2 and 4 hours.

affected by the surfactant HLB values.[42] Nonionic surfactants may also enhance the skin drug permeation by interaction and binding with skin keratin filaments, which may result in disruption within the corneocyte.[43]

Statistical analysis of the obtained results also indicated that the surfactant percent (X_2) has an antagonistic effect on Y_1: A cumulative DPX percent of 49.81% was released when 1% of surfactant was incorporated while 83% DPX was released from films with 0.2% surfactant. This finding could be attributed to the accumulation, and consequently, the formation of a surfactant barrier layer between the film and the skin subcutaneous layer upon further addition of the surfactant. At low concentrations, surfactant molecules increase the permeability of many drugs to the skin, probably due to enhancing penetration and disruption of the skin barrier function.[40] Jantharaprapap and Stagni stated that at high surfactant concentrations, the formation of micelles in the vehicle is more likely to occur and so the amphiphile will trap the permeant and decrease permeability.[44] Shokri et al have studied the surfactant effect on the skin penetration of diazepam and reported similar findings.[45]

Effect of the independent variables on percent elongation (Y_2). The results obtained for the elongation percent (Y_2) of the prepared DPX-loaded transdermal films were in the range of 25% to 50%. It was indicated from the ANOVA that the percent of surfactant (X_2) was agonistically affecting Y_2 at a P value of .0361. This effect is graphically illustrated in the Pareto chart

and the estimated response surface plot of Figure 8. The equation that best describes the model was found to be:

$$Y_2` = 14.1049 + 2.67309 \times X_1` + 9.43341 \times X_2` - 0.0436719 \times X_1`^2 - 2.92056 \times X_1`X_2` + 31.25 \times X_2`^2 \quad \text{(Equation4)}$$

An enhancement in the film's elongation percent upon increasing the nonionic surfactant percent could be attributed to the surfactant plasticizing effect on the film-forming polymer. This explanation was previously illustrated by Eckersley and Rudin, for the effect of the nonionic surfactant (nonylphenol ethylene oxide) on films prepared using acrylic latex polymer.[46]

Preparation and characterization of the optimized DPX film. Based on the multiple response statistical analysis for the data obtained for $Y_1`$ and $Y_2`$, an optimized DPX transdermal film formulation was proposed. This optimum formulation was prepared and the cumulative drug release and elongation percent were tested, as previously described. The optimum levels for $X_1`$ and $X_2`$ were found to be 4.3 and 1%, respectively. The observed values for $Y_1`$ and $Y_2`$ were 78.3% and 55%, respectively. The predicted values for $Y_1`$ and $Y_2`$ were 74.04 and 53.92%, respectively.

The pure drug-loaded transdermal film, which contains the optimized levels of $X_1`$ and $X_2`$, demonstrated values of 52.02% and 50% for $Y_1`$ and $Y_2`$, respectively, a result that indicates the superiority of the film containing DPX PNPs.

Fluorescence Laser Microscopy Test

The transport of pure FITC (control) and the fluorescence-labeled PNPs formulation, from the optimized transdermal film, is illustrated in Figure 9. Unlike the pure FITC, the PNPs formulation was able to transport across the skin SC and viable epidermis during the first 2 hours, and deep to the dermis and other sublayers after 4 hours. This effect was indicated by the intensity of fluorescence. The diffusion of pure FITC was restricted to the upper skin layer. These results indicate successful delivery of the PNPs formulation to deeper skin layers. The fluorescence of the dye was not seen after 1 hour. Limited fluorescence was observed after 2 hours while some fluorescence was observed in the upper skin layers after 4 hours. Our result is in good agreement with previous reports indicated the effectiveness of nanocarrier systems, such as ethosomes and liposomes, in the skin permeation and delivery.[23,47]

Previous studies reported development of different DPX nanocarriers to improve the drug bioavailability. Abourehab et al prepared DPX-loaded polymeric micelles using poly(ethylene glycol) methyl ether-block-poly(lactide-co-glycolide) copolymer. Authors studied the ex vivo permeation across bovine intestine, and the plasma and brain pharmacokinetics following an oral administration of the prepared formulation to Wistar rats. They reported a sustained ex vivo release pattern from the prepared formulation. Moreover, they mentioned that the drug-loaded polymeric micelles enhanced the extent and rate of DPX absorption, prolonged the drug blood circulation time, enhanced the brain DPX accumulation, and increased the drug cerebral concentration.[22] El-Say et al developed Zein-α lipoic acid NPs loaded with DPX to enhance the drug bioavailability and to decrease dosing and side effect. They compared the pharmacokinetics parameters of the prepared formulation with a marketed oral drug tablets on healthy human male volunteers. They reported an increase in the relative bioavailability by 194% from the prepared formulation when compared to the marketed drug product.[48] In this study, the prepared DPX PNPs formulation is similar to the abovementioned NPs in terms of size and drug load. Our optimized transdermal film loaded with DPX PNPs could be considered as a superior DPX drug delivery system due to avoiding of the drug first-pass effect from the transdermal route. This effect is expecting to augment the bioavailability, but a pharmacokinetics study is required.

Conclusions

Two-step optimization was successfully implemented to develop an optimized transdermal film loaded with DPX CS-ALG PNPs. The prepared film extended the drug release, showed an enhanced DPX skin permeation parameters, and was able to penetrate to the deep skin layers. Our DPX PNPs formulation is similar to previously reported DPX NPs, while the prepared transdermal films loaded with DPX PNPs is a promising drug delivery system. The developed drug-PNPs loaded transdermal film is expected to avoid the hepatic first-pass metabolism; as a result, it will significantly improve the bioavailability of DPX in the treatment of PE, but a pharmacokinetics study is required.

Acknowledgment

The authors, therefore, acknowledge with thanks DSR for technical and financial support.

Declaration of Conflicting Interests

The author(s) declared no potential conflicts of interest with respect to the research, authorship, and/or publication of this article.

Funding

The author(s) disclosed receipt of the following financial support for the research, authorship, and/or publication of this article: This project was funded by the Deanship of Scientific Research at King Abdulaziz University, Jeddah, under grant no (RG-6-166-40).

ORCID iD

Tarek A. Ahmed https://orcid.org/0000-0002-9247-4400

References

1. Ahmad MU, Ali SM, Ahmad I. Applications of nanotechnology in pharmaceutical development. In: Moghis Ahmad U, ed. *Lipids in Nanotechnology*. Elsevier; 2012; 171-190. doi:10.1016/B978-0-9818936-7-9.50010-X
2. Buzea C.Nanomaterials and nanoparticle: sources and toxicity. *Biointerphases*. 2007;2(4):17-71. doi:10.1116/1.2815690

3. Soppimath KS, Aminabhavi TM, Kulkarni AR. Biodegradable polymeric nanoparticles as drug delivery devices. *J Control release*. 2001;70(1-2):1-20.
4. Sunderland CJ, Steiert M, Talmadge JE, Derfus AM, Seb A. Targeted nanoparticles for detecting and treating cancer. *Drug Dev Res*. 2006;93(3):70-93. doi:10.1002/ddr
5. Sutradhar KB, Amin L. Nanotechnology in cancer drug delivery and selective targeting. *Int Sch Res Not Nanotechnol*. 2014; 2014:1-12.
6. Panyam J, Labhasetwar V. Biodegradable nanoparticles for drug and gene delivery to cells and tissue ☆. *Adv Drug Deliv Rev*. 2012;64(1):61-71. doi:10.1016/j.addr.2012.09.023
7. Mohanraj VJ, Chen Y. Nanoparticles—a review. *Trop J Pharm Res*. 2006;5(1):561-573.
8. Troncarelli MZ, Brandão HM, Gern JC, Guimarães AS, Langoni H. Nanotechnology and antimicrobials in veterinary medicine. *Microbial Pathogens and Strategeies for Combating Them: Science, Technology and Education*; 2013:543-556.
9. Kumari A, Yadav SK, Yadav SC. Biodegradable polymeric nanoparticles based drug delivery systems. *Colloids Surfaces B Biointerfaces*. 2010;75(1):1-18. doi:10.1016/j.colsurfb.2009.09.001
10. Yang Z, Ma Y, Zhao H, Yuan Y, Kim BYS. Nanotechnology platforms for cancer immunotherapy. *WIREs Nanomed Nanobiotechnol*. 2020;12(2):9. doi:10.1002/wnan.1590
11. Kang C, Sun Y, Zhu J, et al. Delivery of nanoparticles for treatment of brain tumor. *Curr Drug Metab*. 2016;17(8):745-754. doi: 10.2174/1389200217666160728152939
12. Raza R, Mittal A, Kumar P, Alam S, Prakash S, Chauhan N. Approaches and evaluation of transdermal drug delivery system. *Int J Drug Dev Res*. 2015;7(1):222-233.
13. Singh A, Bali A. Formulation and characterization of transdermal patches for controlled delivery of duloxetine hydrochloride. *J Anal Sci Technol*. 2016;7(1):25-38. doi:10.1186/s40543-016-0105-6
14. Prausnitz MR, Langer R. Transdermal drug delivery. *Nat Biotechnol*. 2009;26(11):1261-1268. doi:10.1038/nbt.1504.Transdermal
15. Pastore MN, Kalia YN, Horstmann M, Roberts MS. Transdermal patches: history, development and pharmacology. *Br J Pharmacol*. 2015;172(9):2179. doi:10.1111/BPH.13059
16. Patil RB, Deshmukh TA, Patil VR. Stability indicating HPLC method for dapoxetine HCL in bulk and in formulation. *Int J Pharm Pharm Sci*. 2014;6(5):687-690.
17. Russo A, Capogrosso P, Ventimiglia E, Croce GLA, Boeri L, Montorsi F. Efficacy and safety of dapoxetine in treatment of premature ejaculation: an evidence-based review. *Int J Clin Pract*. 2016;70(9):723-733. doi:10.1111/ijcp.12843
18. Fouad SA, Shamma RN, Basalious EB, El-nabarawi MA, Tayel SA. Novel instantly-soluble transmucosal matrix (ISTM) using dual mechanism solubilizer for sublingual and nasal delivery of dapoxetine hydrochloride: in-vitro / in- vivo evaluation . *Int J Pharm Pharm*. 2016;505(1-2):1-408. doi:10.1016/j.ijpharm.2016.04.006
19. Kashyap R, Srinivasa U, Badodaria K. Development and validation of RP-HPLC method for simultaneous estimation of avanafil and dapoxetine hydrochloride in bulk and dosage form. *World J Pharm Pharm Sci*. 2014;3(7):1697-1719.
20. Giuliano F. A novel treatment of premature ejaculation. *J Eur Assoc Urol*. 2007;6(13):780-786. doi:10.1016/j.eursup.2007.04.005
21. Andersson KE, Mulhall JP, Wyllie M. Pharmacokinetic and pharmacodynamic features of dapoxetine, a novel drug for 'ondemand' treatment of. *Br J Urol Int*. 2006;97(2):311-315. doi:10.1111/j.1464-410X.2006.05911.x
22. Abourehab M, Ahmed O, Balata G, Almalki W. Self-assembled biodegradable polymeric micelles to improve dapoxetine delivery across the blood–brain barrier. *Int J Nanomedicine*. 2018;13(2): 3679-3687. doi:10.2147/IJN.S168148
23. Kurakula M, Ahmed OAA, Fahmy UA, Ahmed TA. Solid lipid nanoparticles for transdermal delivery of avanafil: optimization, formulation, in-vitro and ex-vivo studies. *J Liposome Res*. 2016; 26(4):9. doi:10.3109/08982104.2015.1117490
24. Ahmed TA, El-Say KM. Transdermal film-loaded finasteride microplates to enhance drug skin permeation: two-step optimization study. *Eur J Pharm Sci*. 2016;88:246-256. doi:10.1016/j.ejps.2016.03.015
25. Ahmed TA, El-Say KM. Development of alginate-reinforced chitosan nanoparticles utilizing W/O nanoemulsification/internal crosslinking technique for transdermal delivery of rabeprazole. *Life Sci*. 2014;110(1):35-43. doi:10.1016/j.lfs.2014.06.019
26. Danaei M, Dehghankhold M, Ataei S, et al. Impact of particle size and polydispersity index on the clinical applications of lipidic nanocarrier systems. *Pharmaceutics*. 2018;10(2):57. doi:10.3390/pharmaceutics10020057
27. Ahmed TA, Badr-Eldin SM, Ahmed OAA, Aldawsari H. Intranasal optimized solid lipid nanoparticles loaded in situ gel for enhancing trans-mucosal delivery of simvastatin. *J Drug Deliv Sci Technol*. 2018;48(7):499-508. doi:10.1016/J.JDDST.2018.10.027
28. Bhunchu S, Rojsitthisak P, Rojsitthisak P. Effects of preparation parameters on the characteristics of chitosan-alginate nanoparticles containing curcumin diethyl disuccinate. *J Drug Deliv Sci Technol*. 2015;28(1):64-72. doi:10.1016/j.jddst.2015.05.010
29. Ramin B, Li Y, Jin W, An Y, He L, Li Z. Preparation and optimization of Pickering emulsion stabilized by chitosan-tripolyphosphate nanoparticles for curcumin encapsulation. *Food Hydrocoll*. 2016;52:369-377. doi:10.1016/j.foodhyd.2015.07.015
30. Gazori T, Khoshayand MR, Azizi E, Yazdizade P, Nomani A, Haririan I. Evaluation of alginate/chitosan nanoparticles as antisense delivery vector: formulation, optimization and in vitro characterization. *Carbohydr Polym*. 2009;77(3):599-606. doi:10.1016/j.carbpol.2009.02.019
31. Stoica R, Ion RM. Preparation of chitosan-tripolyphosphate nanoparticles for the encapsulation of polyphenols extracted from rose hips. *Dig J Nanomater Biostructures*. 2013;8(3): 955-963.
32. Attia AK, Souaya ER, Soliman EA. Thermal analysis investigation of dapoxetine and vardenafil hydrochlorides using molecular orbital calculations. *Adv Pharm Bull*. 2015;5(4):523-529. doi:10.15171/apb.2015.071
33. Fouad SA, Shamma RN, Basalious EB, El-Nabarawi MM, Tayel SA. Novel instantly-dispersible nanocarrier powder system (IDNPs) for intranasal delivery of dapoxetine hydrochloride:

in-vitro optimization, *ex-vivo* permeation studies, and *in-vivo* evaluation. *Drug Dev Ind Pharm*. 2018;44(9):1443-1450. doi: 10.1080/03639045.2018.1459675

34. Crcarevska MS, Dodov MG, Goracinova K. Chitosan coated Ca—alginate microparticles loaded with budesonide for delivery to the inflamed colonic mucosa. *Eur J Pharm Biopharm*. 2008; 68(3):565-578. doi:10.1016/j.ejpb.2007.06.007
35. Soliman SM, Elagizy HMY, El A. Validated stability-indicating derivative spectrophotometry and synchronous fluorescence spectroscopy methods for the determination of dapoxetine hydrochloride in the presence of its degradation product and co-formulated drugs. *Pharm Anal Acta*. 2017;8(10):2153-2435. doi:10.4172/ 2153-2435.1000564
36. Sankalia MG, Mashru RC, Sankalia JM, Sutariya VB. Reversed chitosan–alginate polyelectrolyte complex for stability improvement of alpha-amylase: optimization and physicochemical characterization. *Eur J Pharm Biopharm*. 2007;65(2):215-232. doi:10. 1016/j.ejpb.2006.07.014
37. Sartori C, Finch DS, Ralph B, Gilding K. Determination of the cation content of alginate thin films by FTi.r. spectroscopy. *Polymer (Guildf)*. 1997;38(1):43-51. doi:10.1016/S0032-3861(96)00458-2
38. Som I, Bhatia K, Yasir M. Status of surfactants as penetration enhancers in transdermal drug delivery. *J Pharm Bioallied Sci*. 2012;4(1):2-9. doi:10.4103/0975-7406.92724
39. Chen L, Tan F, Wang J, Liu F. Assessment of the percutaneous penetration of indomethacin from soybean oil microemulsion: effects of the HLB value of mixed surfactants. *Int J Pharm Sci*. 2012;67(1):31-36. doi:10.1691/ph.2012.1085.
40. Som I, Yasir M. Status of surfactants as penetration enhancers in transdermal drug delivery. *J Pharm Bioallied Sci*. 2012;4(1):2-9. doi:10.4103/0975-7406.92724.
41. Wu H, Ramachandran C, Weiner ND, Roessler BJ. Topical transport of hydrophilic compounds using water-in-oil nanoemulsions. *Int J Pharm*. 2001;220(1-2):63-75.
42. Cho HK, Cho JH, Choi S, Cheong IW. Topical delivery of retinol emulsions co-stabilised by PEO-PCL- PEO triblock copolymers: effect of PCL block length. *J Microencapsul*. 2012;29(8):1-8. doi: 10.3109/02652048.2012.686528
43. Nokhodchi A, Shokri J, Dashbolaghi A, Hassan-Zadeh D, Ghafourian T, Barzegar-Jalali M. The enhancement effect of surfactants on the penetration of lorazepam through rat skin. *Int J Pharm*. 2003;250(2):359-369. Accessed March 17, 2019. http://www.ncbi.nlm.nih.gov/pubmed/12527163
44. Jantharaprapap R, Stagni G. Effects of penetration enhancers on in vitro permeability of meloxicam gels. *Int J Pharm*. 2007;343(1-2):26-33. doi:10.1016/j.ijpharm.2007.04.011
45. Shokri J, Nokhodchi A, Dashbolaghi A, Hassan-zadeh D. The effect of surfactants on the skin penetration of diazepam. *Int J Pharm*. 2001;228(1-2):99-107.
46. Eckersley ST, Rudin A. The effect of plasticization and pH on film formation of acrylic latexes. *J Appl Polym Sci*. 1993;48(8): 1369-1381. doi:10.1002/app.1993.070480805
47. Ahmed TA, El-Say KM, Aljaeid BM, Fahmy UA, Abd-Allah FI. Transdermal glimepiride delivery system based on optimized ethosomal nano-vesicles: preparation, characterization, in vitro, ex vivo and clinical evaluation. *Int J Pharm*. 2016;500(1-2):245-254. doi:10.1016/j.ijpharm. 2016.01.017
48. Khalid El-Say M, Osama Ahmed A, Amir Mohamed I, Martin Safo K, Abdelsattar Omar M. Zein-alpha lipoic acid-loaded nanoparticles to enhance the oral bioavailability of dapoxetine: optimization and clinical pharmacokinetic evaluation. *Int J Nanomedicine*. 2019;14:7461-7473.